

## **DMO and NMO as applied in seismic data processing**

JUNNYIH CHEN

Chinese Petroleum Corporation,  
4-7F, No. 53, Jen Ai Rd., Sec. 3,  
Taipei, Taiwan, 10628 R.O.C.

**Abstract :** DMO (dip-moveout) is recognized as the technique to image the steep dip events which are indiscriminately smeared when the data are processed with the conventional seismic imaging method, which includes NMO, CMP stacking and zero offset migration. From these published papers, we may find many ways to do DMO, such as prestack partial migration, DMO by Fourier transform, offset continuation, single channel DMO... etc, and the improvements of these techniques are widely recognized. But every technique is available only in two-dimensional case.

To extend DMO to 3D (three dimensional) case, those techniques operating on constant offset section are generally available only when the feathering angle can be constrained within a very small value, but this condition is really hard to be achieved when the sea current is rough. In this paper the author is going to extend the "Rocca's smile" operator into 3D case, so that an easy way of doing DMO will be available to any 3D data.

A further consideration is also given to mixing the NMO with the DMO in this paper. The reason for doing this is not only to simplify the process and to save computer time, but also to search for more accurate velocity information for the NMO correction when the dip angle is large. This technique will be very effective compared to sole DMO, when the velocity changes very rapidly with depth.

### **INTRODUCTION**

DMO is a well-known technique for imaging steep dip events. Since Yilmaz and Claerbout published their algorithm of prestack partial migration in 1980, alot of work on this topic have been presented by different authors. So far it is known with different technology terms as DEVILISH (Judson *et al.*, 1978), prestack partial migration, offset continuation ( Bolondi, Loinger and Rocca, 1982) and DMO. Almost all of these techniques are working on COS (Constant Offset Section), and subject to the same constraints when extending from 2D (two dimensional) situation to 3D (three dimensional). In data acquisition, normally the feathering angle can be controlled under a very limited angle, that will promise the availability of the 2D DMO to 3D data. But when the feathering angle is not under control and changing from place to place, all these techniques will then sustain unpredictable mistakes.

Biondi and Ronen(1987) tried to project DMO process into shot profiles. This probably will solve the problem of feathering. But when the cable bends into curve and geophones are no more on a straight line, then there will still be the problem for applying shot profile DMO to 3D seismic data.

### 3D DIP MOVEOUT

Deregowski and Rocca(1981) derived the smear-stack operator to map any non-zero offset 2D section to zero offset. To see how can we apply 2D DMO to 3D data, the author simulates the same procedure for the 3D case. In this paper,  $v$  is generally used to denote velocity,  $t_h, t_n, t_z$  and  $t_m$  denote the time scale before NMO, after NMO, after DMO and after migration respectively, and  $h$  represents the half offset.

Suppose that there is a subsurface reflector of an ellipsoid, with its two foci right on our seismic source station and receiver station. With the characteristics of ellipsoid, when a pulse comes out from one of the two foci, it will then arrive at the other focus concentrically after being reflected by the ellipsoid reflector. This implies that there exists a spike on the trace with offset  $2h$  at time  $t_h$ , and  $vt_h$  is equal to the distance between A and B as shown in Figure 1.

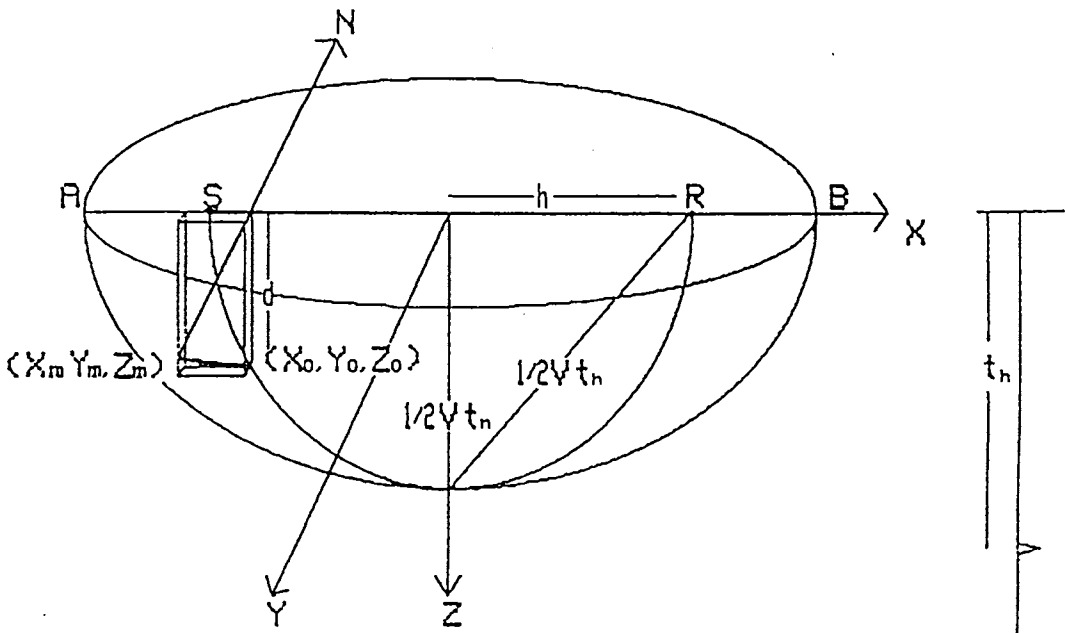


Figure 1 : Ellipsoid reflector

For conventional seismic data processing, this spike is then NMO corrected to time

$$t_n^2 = \sqrt{t_h^2 + 4h^2v^{-2}} \quad (1)$$

and CMP stacked to the zero offset section. After stacking, this spike will then be zero offset migrated to a hemisphere with radius  $vt_n$ . That means that for a spike on the non-zero offset trace, the conventional processing has generated a result of hemisphere with radius  $vt_n$ , while the actual reflector is an ellipsoid. In order to have the ellipsoid as the final result of zero offset migration, what should be the impulse response of this spike before migration? A simple way to get the answer is but to inversely migrate the ellipsoid and see what is the result. The anticipated ellipsoid can be defined as

$$\frac{x^2}{a^2} + \frac{y^2}{b^2} + \frac{z^2}{b^2} = 1 \quad (2)$$

where  $a = 1/2 vt_n$ ,  $b = 1/2 vt_n = \sqrt{a^2 - h^2}$

To inversely migrate the ellipsoid, an arbitrary point  $(x_m, y_m, z_m)$  is selected on this ellipsoid and the line which contains this point and normal to the ellipsoid has to be found out. Since the slope tangential to the ellipsoid is

$$\left. \frac{\partial z}{\partial x} \right|_{x_m, z_m} = \left. \frac{-b^2 x}{a^2 z} \right|_{x_m, z_m} = \frac{-b^2 x_m}{a^2 z_m} \quad (3)$$

$$\left. \frac{\partial z}{\partial y} \right|_{y_m, z_m} = \left. \frac{-y}{z} \right|_{y_m, z_m} = \frac{-y_m}{z_m} \quad (4)$$

the line normal to this ellipsoid can be written as

$$\frac{z - z_m}{x - x_m} = \frac{a^2 z_m}{b^2 x_m} \quad (5)$$

$$\frac{z - z_m}{y - y_m} = \frac{z_m}{y_m}$$

This normal line intersects the surface plane at  $z = z_s = 0$ . By inserting  $z = 0$  into (5),  $x_s$  and  $y_s$  can be found to be

$$x_s = \frac{b^2 x_m}{a^2} + x_m \quad (6)$$

$$y_s = 0$$

The distance between  $(x_m, y_m, z_m)$  and  $(x_s, y_s, 0)$  can then be calculated via equation

$$d = \sqrt{y_m^2 + z_m^2 + (x_s - x_m)^2} \quad (7)$$

3D inverse migration is but to move the energy from  $(x_m, y_m, z_m)$  to  $(x_o, y_o, z_o)$ , where

$$x_o = x_s = \frac{b^2 x_m}{a^2} + x_n \quad (8)$$

$$y_o = y_s = 0 \quad (9)$$

$$\text{and } z = d = \sqrt{y_m^2 + z_m^2 + (x_s - x_m)^2} \quad (10)$$

Since  $x_m, y_m, z_m$  are coordinates of a point on the surface of ellipsoid, they must be subjected to the condition

$$\frac{x_m^2}{a^2} + \frac{y_m^2}{b^2} + \frac{z_m^2}{b^2} = 1 \quad (11)$$

By inserting (10) into (11) to eliminate  $z_m$ ,

$$\frac{z_o^2}{b^2} = 1 - \frac{x_m^2}{a^2} + \frac{(x_o - x_m)^2}{b^2} \quad (12)$$

To eliminate  $x_m$ , replacing  $x_m$  in equation (8), the relationship between  $x_o, y_o$  and  $z_o$  is now in the form of

$$\frac{z_o^2}{b^2} + \frac{x_o^2}{a^2 - b^2} = 1$$

as a result

$$\frac{t_z^2}{t_n^2} = \frac{x_o^2}{h^2} = 1 \quad (13)$$

Ellipse (13) is the same as the "Rooca smile" of 2D DMO. That means that 3D DMO impulse response is completely the same as that of 2D DMO; the only difference is that, 3D DMO keeps it's smile right on the plane of  $y = 0$  (verticle plane contains source and receiver), while 2D data automatically have smiles on this plane. This explains why 2D DMO is able to be applied as 3D DMO, when the 3D data are collected with regular 2D lines.

### DMO AND NMO

Normally an approximate NMO correction is required before applying DMO. One of the problem of NMO before DMO is that, velocity for NMO is not the same velocity for migration, when reflectors are not completely horizontal. This can be understood from Figure 1, the velocity corresponding to the ray from source to reflector and to receiver is a function of  $t_m$  (migrated time scale that corresponds to depth). But when doing NMO, it's still too early to know  $t_n$  and also  $v(t_m)$ . Since  $t_n$ , time after NMO, is unequal to  $t_n$  for the dipping events, conventionally using velocity  $v(t_n)$  for NMO implies that zero dip is always assumed.

Actually this problem can easily be solved by doing NMO and DMO simultaneously if the lateral velocity change is negligible. In order to do that an approximate velocity as a function of  $t_m$  is assumed to be known. With the annotation of  $h$  as the half offset and  $x_0$  as the distance between CMP (Common Middle Point) and CRP (Common Reflection Point), their NMO, DMO and migration relationships can be easily built as

$$t_h^2 = t_n^2 + \frac{h^2}{v^2} \quad (14)$$

$$\frac{t_z^2}{t_n^2} + \frac{x_0^2}{h^2} = 1 \quad (15)$$

and

$$\begin{aligned} t_m &= t_z \cos^2 \theta_m = t_z \sqrt{1 - \sin^2 \theta_m} \\ &= t_z \sqrt{1 - \tan^2 \theta_0} \\ &= t_z \sqrt{\left[1 - \left(\frac{v dt_z}{dx_0}\right)^2\right]} \end{aligned} \quad (16)$$

where  $\theta_m$  denotes the dip angle of reflectors,  $\theta_0$  denotes the apparent dip of events before migration. In equation (16)  $dt_z/dx_0$  relates to  $\tan \theta_0$  and can be derived from equation (15) as

$$\frac{dt_z}{dx_0} = -\frac{1}{2} \frac{t_n^2 x_0}{h^2 t_z} \quad (17)$$

By inserting (17) into (16), then

$$t_n = \sqrt{t_z \left[1 - \frac{v^2 x_0^2 t_z^2}{4(h^2 - x_0^2)^2}\right]^2} \quad (18)$$

Since DMO and NMO are to be done simultaneously, the relationship between  $t_z$  and  $t_n$  has to be set up. With the help of these equations, the algorithm of following chart (Figure 2) gives the way for getting  $t_n = t_n(t_z, h, x_0)$

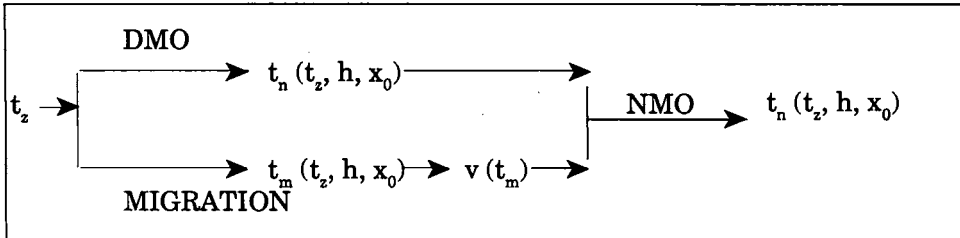


**Figure 2 :** Given  $t_z$ ,  $t_n$  and  $t_m$  are known from Equation (15) and (18) respectively, and  $v(t_m)$  is chosen after  $t_m$  is known. Finally with Equation (14),  $t_n$  is obtained for this  $t_z$ .

For any specific  $t_z$ ,  $t_n$  can be calculated from Equation (15), and  $t_m$  can be obtained with Equation (18). Then the velocity  $v(t_m)$  can be chosen. Once  $v$  and  $t_n$  are known,  $t_z$  is fixed according to Equation (14).

One problem of computing  $t_m$  with equation (18) is that,  $v(t_m)$  has to be known before calculating  $t_m$ . It seems that there is no exact solution. In practice, it's always viable to get a very close value  $v(t_m)$  for calculating  $t_m$ . Since velocity normally would not change much between consecutive grid points, we can approach it by starting from  $t_m = 0$  when  $t_z = 0$  and  $v = v(0)$ , and this velocity is used to replace  $v(t_m)$  in equation for calculating  $t_m(t_z = dt)$ . That means for calculating  $t_m$  to get  $v(t_m(t_z))$ , we always use the velocity value of the previous step  $v(t_m(t_z - dt))$ . This sufficiently promises the accuracy of velocity function to be used.

Once this relation is set then DMO with NMO is merely a process of swing each spike into a smile specified as  $t_z - t_n$  relation according to different  $h$  and  $x_0$ . For more general cases when curved ray path are required to be considered, a  $t_z - t_n$  table can be obtained by ray tracing method after  $t_m$  is known. This means DMO is no longer based on the constant velocity model. In this paper, the author simply thinks that constant velocity model is accurate enough for reflection seismology.

Figure 3 shows the velocity model for one point scatterer located at the middle of this section, the time depth of this point is assumed to be 400msec. Figure 4 and 5 are the constant offset sections corresponding to  $h=0$  m and 500 m respectively. Figure 6 shows superior result of DMO with NMO while figure 7 shows the DMO after NMO result, since figure 6 is more similar to the zero offset section of Figure 4.

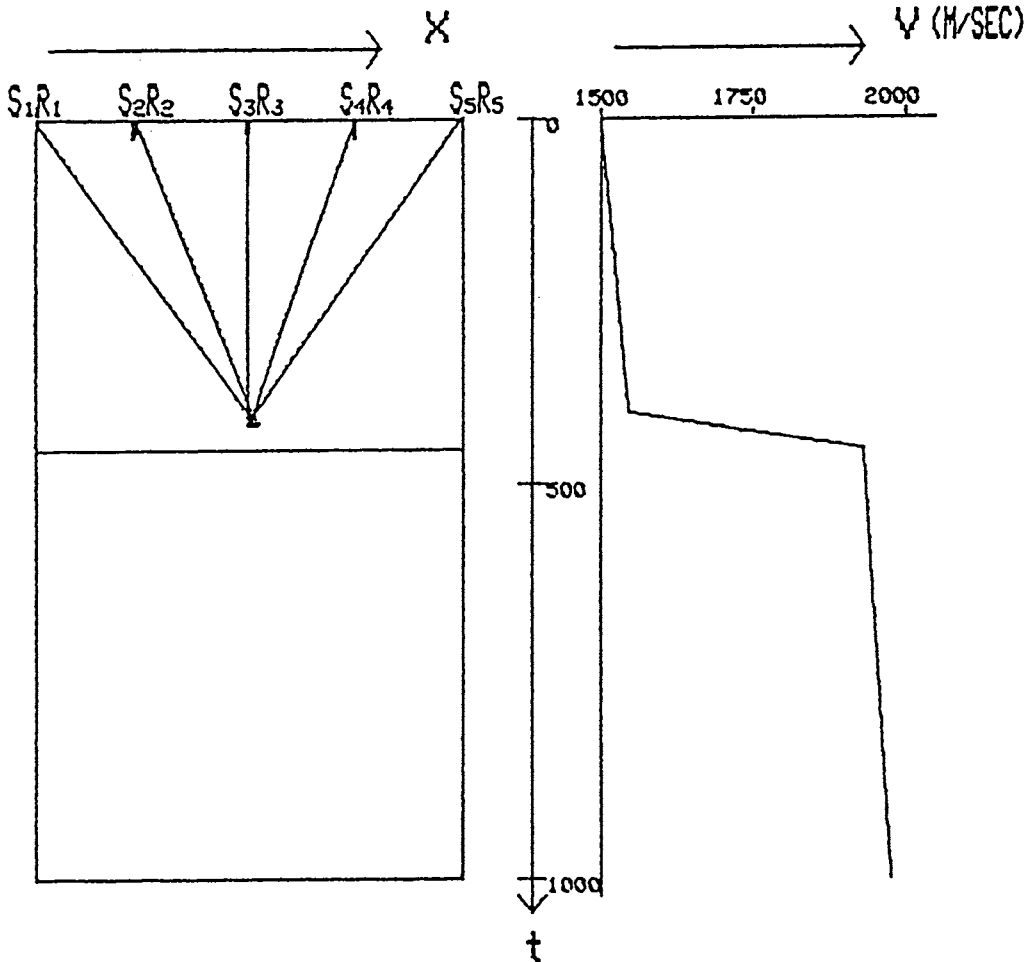


Figure 3 : Velocity model

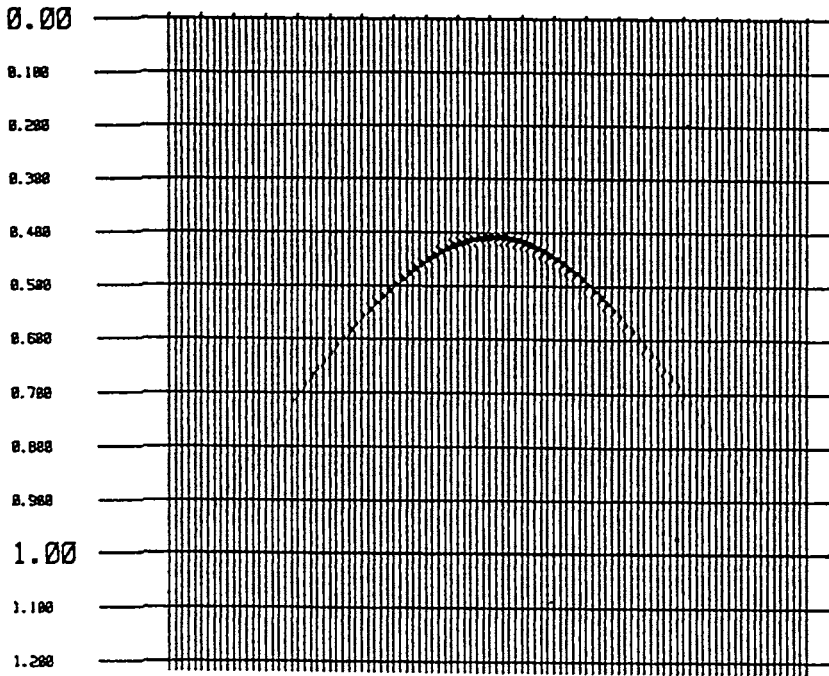


Figure 4 : Zero offset section

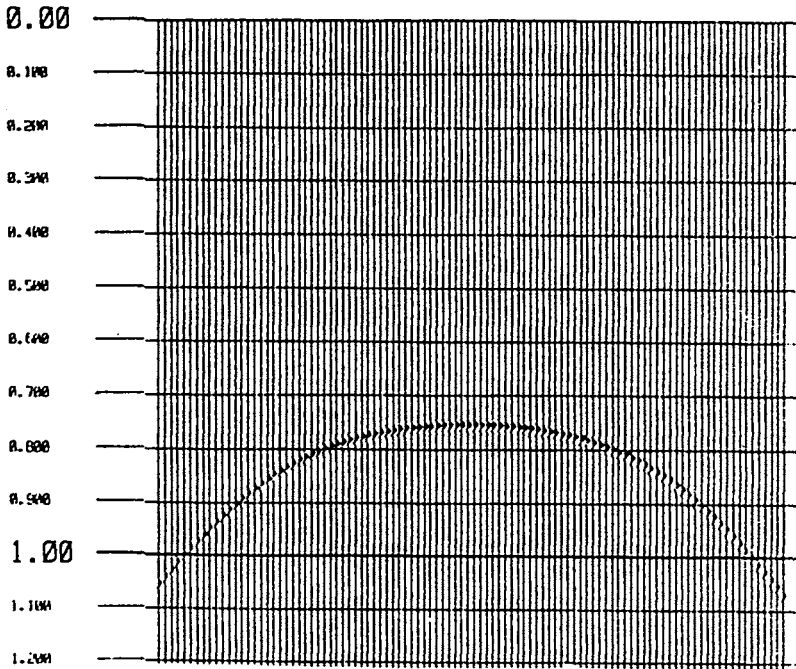


Figure 5 : COG (constant offset gather) with  $h = 1000$  m

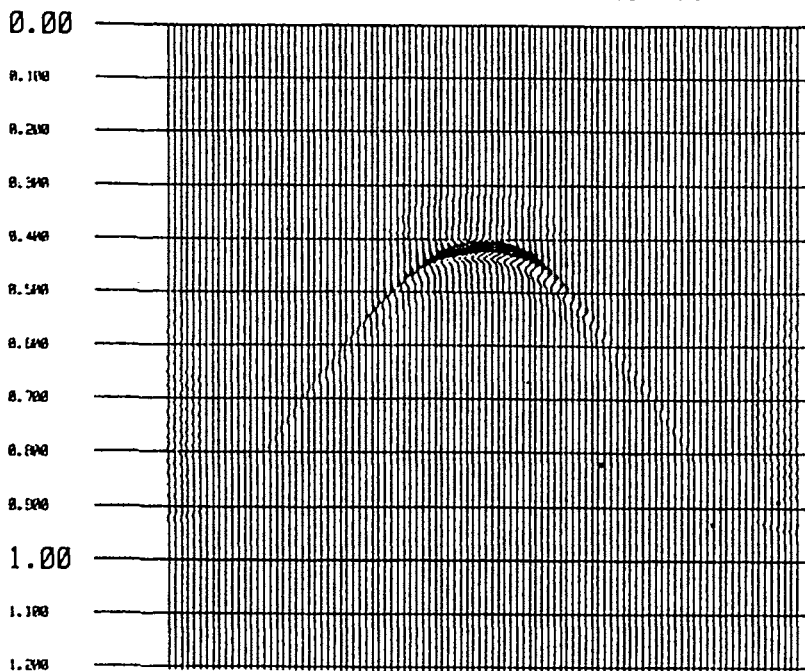


Figure 6 : COG section after combining DMO and NMO

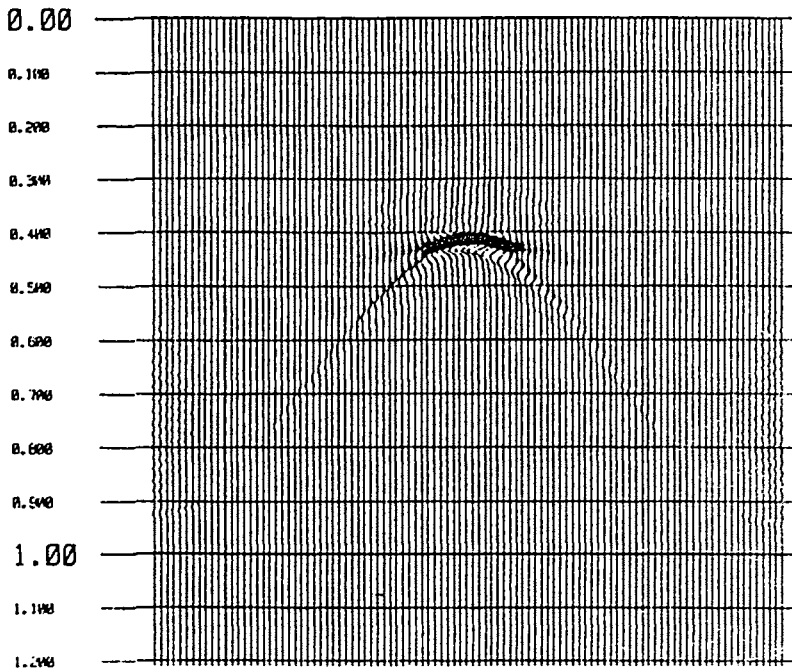


Figure 7 : COG section when DMO and NMO are processed individually

With this new technique, we processed a marine section. Figure 8 shows the conventional processing result, Figure 9 shows the result where DMO is applied after NMO while Figure 10 shows the result where DMO and NMO have been combined to one operation. From these figures the difference between conventional section and DMO section can be clearly seen, but the difference between Figures 9 and 10 is not so obvious, that's because in this area, vertical velocity variation is not serious. But if we look into the very shallow part of Figures 9 and 10, there can be seen some improvements, because in this very shallow zone, NMO is very sensitive to the accuracy of velocity.

### CONCLUSIONS

1. DMO is a very efficient means in imaging high steep events.
2. When 3D data are composed of 2D lines with regular geometry, conventional 2D DMO can be applied to the individual lines to achieve 3D DMO result.
3. Serious vertical velocity variation will affect the effectiveness of DMO. In such a case, DMO and NMO should be combined into one operation, so that more accurate velocity is able to be used for NMO correction to enhance the effectiveness of DMO.

### ACKNOWLEDGEMENTS

The author thanks Dr. Y.S. Pan, Dr. F.C. Su and Mr W.S. Chen for their encouragement and help to complete this paper. This work is supported by Offshore Petroleum Exploration Division, Chinese Petroleum Corp.

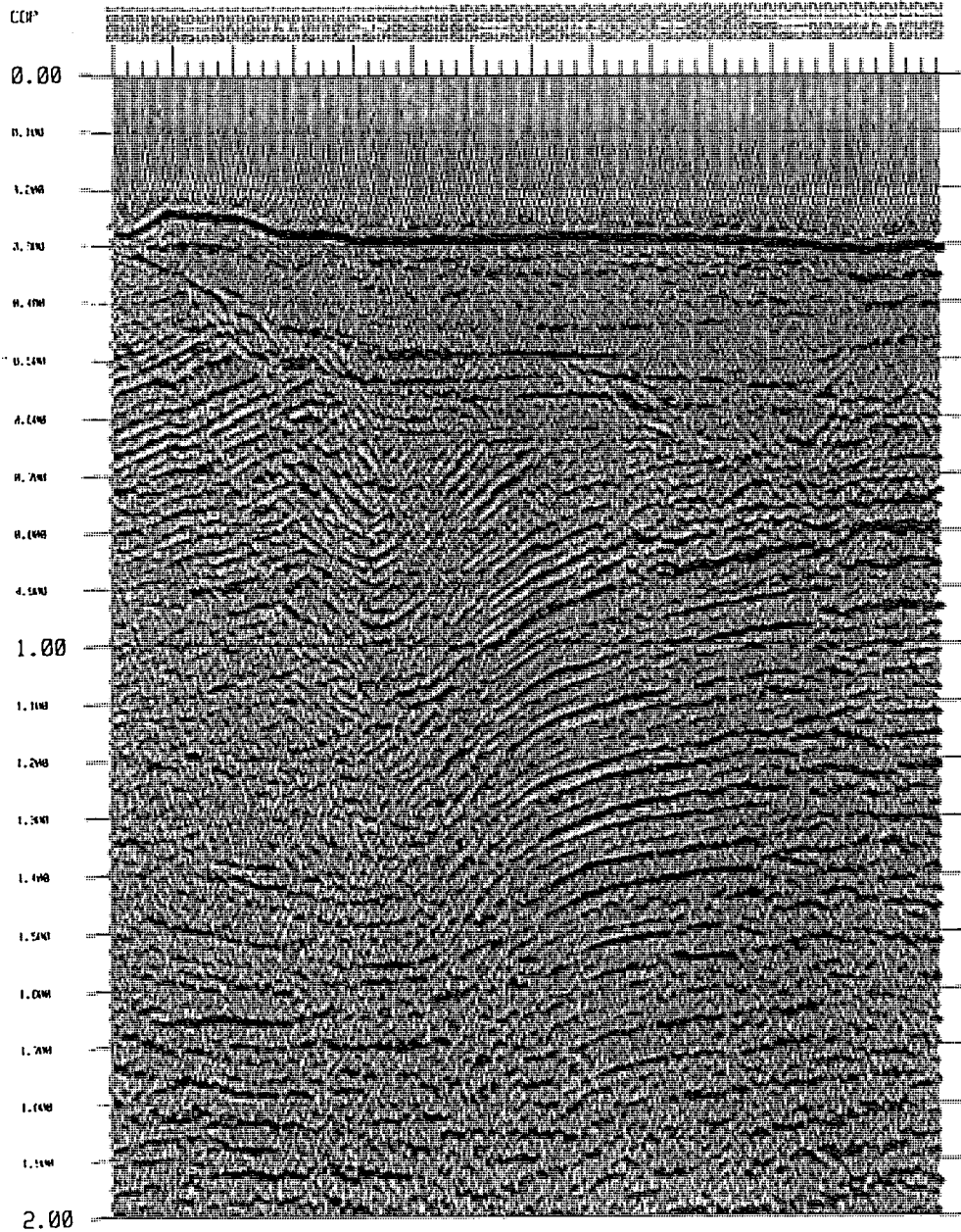


**Figure 8 :** A marine seismic section without applying DMO

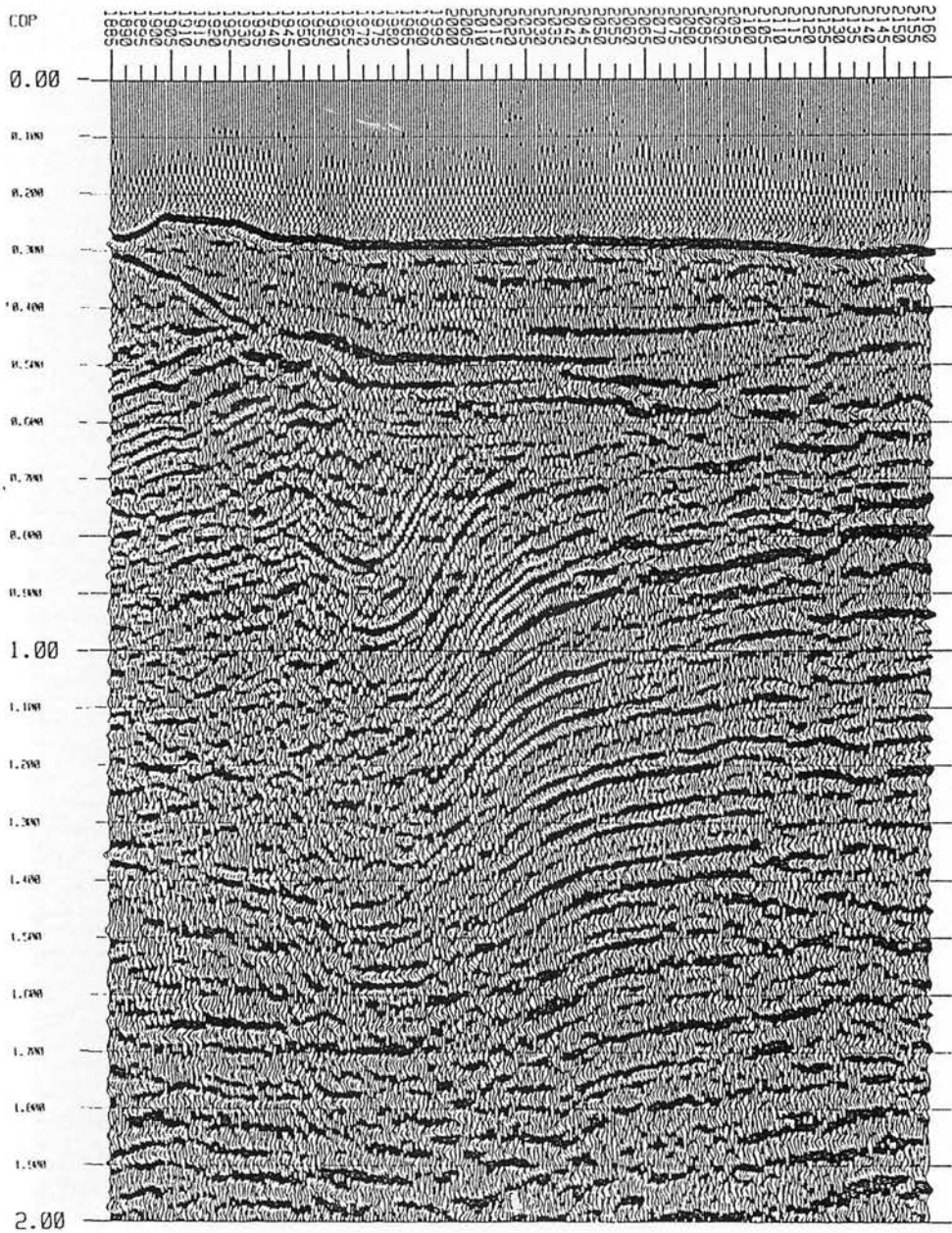
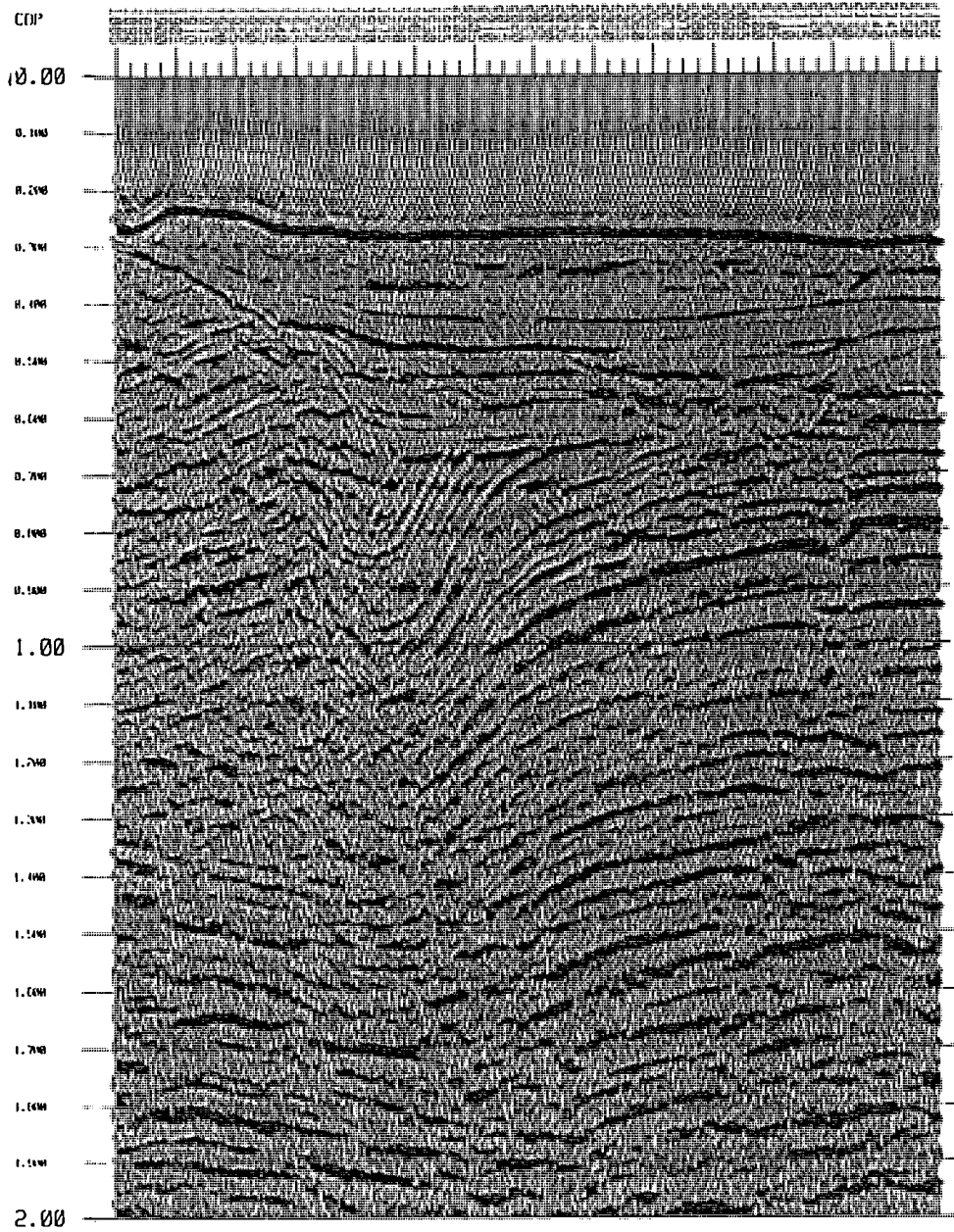


Figure 9 : A marine seismic section when DMO and NMO are applied individually



**Figure 10 :** A marine seismic section when DMO and NMO are combined as one operation

## REFERENCES

- BIONDI, B. and RONEN, J., 1987. Dip move out in shot profile. *Geophysics*, *52*, 1473-1482.
- BOLONDI, G. LOINCER, E. and ROCCA, F., 1982. Offset continuation of seismic sections. *Geophys. Prosp.*, *30*, 813-828.
- BROWN, R. J., 1969. Normal moveout and velocity relations for flat and dipping beds for long offsets. *Geophysics*, *34*, 180-195.
- CLAERBOUT, J.F., 1976. *Fundamentals of geophysical data processing*. New York, McGraw-Hill Book Co., Inc.
- CLAERBOUT, J.F., 1985. *Imaging the earth's interior*. Palo Alto, Blackwell Scientific Publications Book Co.
- CLAERBOUT, J.F., and DOHERTY, S.M., 1972. Downward continuation of moveout corrected seismograms. *Geophysics*, *37*, 741-768.
- DEREGOWSKI, S. M., and ROCCA, F., 1981. Geometrical optics and wave theory of constant offset section in layered media. *Geophys. Prosp.*, *29*, 384-406.
- DIX, C. H., 1955. Seismic velocities from surface measurements. *Geophysics*, *20*, 68-86.
- GAZDAG, J., 1978. Wave equation migration with the phase shift method. *Geophysics*, *43*, 1342-1351.
- HALE, I.D., 1984. Dip-move-out by Fourier transform. *Geophysics*, *49*, 741-757.
- JACOBS, A., 1982. *The prestack migration of shot profile*. Ph.D. Thesis, Stanford University.
- Judson, D.r., Schultz, P.S., and Sherwood, J.W.C., 1978. *Equalizing the stacking velocities of dipping events via Devilish*. Presented at the 48th Annual International SEG Meeting in San Francisco; brochure published by Digicon Geophysical Corp.
- Levin, F.K., 1971. Apparent velocity from dipping interface reflection. *Geophysics*, *36*, 510-516.
- Ottolini, R. and Claerbout, J.F., 1984. The migration of common midpoint slant stack. *Geophysics*, *49*, 237-249.
- Rockwell, D.W., 1971. Migration stack aids interpretation. *Oil and gas, J.*, *69*, no.16, 202-218.
- Sattlegger, J.W., and Stiller, P.K., 1974. Section migration before or after stack. *Geophys. Prosp.*, *22*, 297-314.
- Schultz, P.S., and Sherwood, J.W.C., 1980. Depth migration before stack. *Geophysics*, *45*, 376-393.
- Taner, T.M., and Koehler, F., 1969. Velocity spectra—digital computer derivation and application of velocity functions. *Geophysics*, *34*, 895-881.
- Yilmaz, O., and Claerbout, J.F., 1980. Prestack partial migration. *Geophysics*, *45*, 1753-1779.